Research Paper https://doi.org/10.7733/jnfcwt.2022.036

Spectroscopic Characterization of Aqueous and Colloidal Am(III)-CO_3 Complexes for Monitoring Species Evolution

Hee-Kyung Kim
Korea Atomic Energy Research Institute, 111, Daedeok-daero 989beon-gil, Yuseong-gu, Daejeon 34057, Republic of Korea

(Received July 25, 2022 / Revised September 19, 2022 / Approved September 27, 2022)

Carbonates are inorganic ligands that are abundant in natural groundwater. They strongly influence radionuclide mobility by forming strong complexes, thereby increasing solubility and reducing soil absorption rates. We characterized the spectroscopic properties of Am(III)-carbonate species using UV-Vis absorption and time-resolved laser-induced fluorescence spectroscopy. The deconvoluted absorption spectra of aqueous $Am(CO_3)_2^-$ and $Am(CO_3)_3^{3-}$ species were identified at red-shifted positions with lower molar absorption coefficients compared to the absorption spectrum of aqua Am^{3+}. The luminescence spectrum of $Am(CO_3)_3^{3-}$ was red-shifted from 688 nm for Am^{3+} to 695 nm with enhanced intensity and an extended lifetime. Colloidal Am(III)-carbonate compounds exhibited absorption at approximately 506 nm but had non-luminescent properties. Slow formation of colloidal particles was monitored based on the absorption spectral changes over the sample aging time. The experimental results showed that the solubility of Am(III) in carbonate solutions was higher than the predicted values from the thermodynamic constants in OECD-NEA reviews. These results emphasize the importance of kinetic parameters as well as thermodynamic constants to predict radionuclide migration. The identified spectroscopic properties of Am(III)-carbonate species enable monitoring time-dependent species evolution in addition to determining the thermodynamics of Am(III) in carbonate systems.

Keywords: Americium, Carbonate, Radionuclide migration, Spectroscopy, Thermodynamics, Kinetics

*Corresponding Author.
Hee-Kyung Kim, Korea Atomic Energy Research Institute, E-mail: hkim11@kaeri.re.kr, Tel: +82-42-866-6294

ORCID
Hee-Kyung Kim http://orcid.org/0000-0001-5840-7194

1. Introduction

Assessing the safety of high-level radioactive waste repository systems requires a thorough understanding of the migration behavior of radionuclides in aquatic systems, including in natural groundwater and pore waters of engineering barriers [1]. Carbonate ions are among the most abundant inorganic ligands in natural groundwater and are concentrated in cement pore water. As potent complexing agents, carbonate forms stable bi- and tri-complexes such as $Am(CO_3)_n^{3-2n}$ and $UO_2(CO_3)_n^{2-2n}$ (n = 1–3) according to OECD-NEA chemical thermodynamic reviews [2]. Additionally, anionic carbonate complexes interact with naturally abundant Ca^{2+} to produce ternary complexes including Ca-UO_2-CO_3 and Ca-PuO_2-CO_3 [3-5]. Particularly, $CaUO_2(CO_3)_3^{2-}$ and $Ca_2UO_2(CO_3)_3$(aq) complexes are predicted to be the predominant uranyl species in groundwater [6-9], and these Ca-UO_2-CO_3 ternary carbonate complexes play critical roles in increasing the mobility of uranium, such as by hindering sorption reactions onto soils and minerals [10-11] and inhibiting bacterial reduction of U(VI) to U(IV) [12]. As such, carbonates complicate the chemistry of radionuclides in natural environments, strongly influencing their migration behaviors.

Americium is one of the most concerning radionuclides with respect to the long-term radiotoxicity of spent nuclear fuels [1]. As per OECD-NEA chemical thermodynamics reviews [2, 13], thermodynamic data for aqueous complexes of $Am(CO_3)_n^{3-2n}$ (n = 1–3) and $Am(HCO_3)^{2+}$ were evaluated using various methods, including solvent extraction [14], solubilities [15-16], UV-Vis absorption, laser-induced photoacoustic spectroscopy (LPAS) of Am(III) coupled with solubilities [17-18], time-resolved laser fluorescence spectroscopy (TRLFS) of Cm(III) [15, 19-21], and TRLFS on Eu(III) [19, 22-23]. The relevant complex formation constants and solubility products of Am(III)–CO_3 systems are listed in Table 1. For solid compounds, few studies have been conducted on $AmOHCO_3 \cdot xH_2O$(s), $Am_2(CO_3)_3 \cdot xH_2O$(s), and $NaAm(CO_3)_2 \cdot xH_2O$(s), as discussed in OECD-NEA chemical thermodynamics reviews [2, 13]. Notably, thermodynamic data obtained from solubility studies exhibit large uncertainties arising from uncertainties in the solid phases, such as different degrees of crystallinity, the probable transformation of solid phases by α-irradiation, and partial chemical changes upon hydration in aqueous solutions. These properties are typically challenging to quantitatively characterize. Additionally, amorphous solids often exhibit widely scattered solubility data.

Am(III) shows characteristic absorptions at 503 nm (ε = 424 ± 8 $M^{-1} \cdot cm^{-1}$) and 813 nm (ε = 64–72 $M^{-1} \cdot cm^{-1}$) and luminescence at 688 nm with a lifetime of 23.3 ± 0.4 ns [24-26]. We previously demonstrated that the absorption of Am(III) at 503 nm sensitively changes upon complex formation, enabling speciation and determination of the formation constants [27-28]. In addition, characteristic luminescence property changes detected using TRLFS provide information on the coordination environment of the Am(III) center [27-28]. Few spectroscopic studies have been performed to evaluate Am(III)-carbonate systems. The absorption properties of aqueous $Am(CO_3)^+$, $Am(CO_3)_2^-$, and $Am(CO_3)_3^{3-}$ have been reported in limited LPAS studies [17-18] and the luminescence properties of aqueous $Am(CO_3)_3^{3-}$ and solid compounds of $NaAm(CO_3)_2$(s) and $AmOHCO_3$(s) were reported in a TRLFS study [29]. However, these independent studies were conducted under different experimental conditions, and the results were not subsequently confirmed. Therefore, the absorption and luminescence properties of Am(III)-carbonate samples should be systematically examined under controlled experimental conditions.

In this study, the species distribution of Am(III) in carbonate solutions was simulated based on selected thermodynamic data from OECD-NEA reviews along with experimental measurements. UV-Vis spectrophotometry and TRLFS were employed to characterize the absorption and luminescence properties of aqueous and colloidal Am(III)-CO_3 complexes. The individual absorption spectra of the aqueous Am(III)-CO_3 complexes were identified. Colloidal particle formation was monitored by tracking changes

Table 1. Equilibrium constants of Am(III) complexes involving OH^- and CO_3^{2-}

Aqueous reactions	$\log\beta^0$	$\log\beta$ (1 M $NaClO_4$)
$H^+ + CO_3^{2-} \leftrightarrow HCO_3^-$	10.329 ± 0.02	9.57
$Am^{3+} + CO_3^{2-} \leftrightarrow Am(CO_3)^+$	8.0 ± 0.4	5.80
$Am^{3+} + 2CO_3^{2-} \leftrightarrow Am(CO_3)_2^-$	12.9 ± 0.6	10.11
$Am^{3+} + 3CO_3^{2-} \leftrightarrow Am(CO_3)_3^{3-}$	15.0 ± 0.5	13.04
$Am^{3+} + HCO_3^- \leftrightarrow Am(HCO_3)^{2+}$	3.1 ± 0.3	1.98
$Am^{3+} + H_2O \leftrightarrow Am(OH)^{2+} + H^+$	−7.2 ± 0.5	−8.06
$Am^{3+} + 2H_2O \leftrightarrow Am(OH)_2^+ + 2H^+$	−15.1 ± 0.7	−16.28
$Am^{3+} + 3H_2O \leftrightarrow Am(OH)_3(aq) + 3H^+$	−26.2 ± 0.5	−27.36
Solubility	$\log K_{s,0}^0$	$\log K_{s,0}$ (1 M $NaClO_4$)
$Am_2(CO_3)_3(s, am) \leftrightarrow 2Am^{3+} + 3CO_3^{2-}(aq)$	−33.4 ± 2.2	−32.72
$AmOHCO_3(am, hyd) + H^+ \leftrightarrow Am^{3+} + CO_3^{2-} + H_2O$	−6.199 ± 1.0	−4.01
$AmOHCO_3 \cdot 0.5H_2O(cr) + H^+ \leftrightarrow Am^{3+} + CO_3^{2-} + 1.5H_2O$	−8.40 ± 1.0	−6.20
$NaAm(CO_3)_2 \cdot 5H_2O(cr) \leftrightarrow Na^+ + Am^{3+} + 2CO_3^{2-} + 5H_2O$	−21 ± 0.5	−17.73
$Am(OH)_3(s, am) + 3H^+ \leftrightarrow Am^{3+} + 3H_2O$	16.9 ± 0.8	18.06

The equilibrium constants under standard conditions (I = 0) were converted to those in I = 1 M $NaClO_4$ according to the specific ion interaction theory.

in the absorption spectra. The slow formation of colloidal particles and solid compounds was monitored based on the characteristic changes in the absorption spectra with the sample aging time.

2. Methods

2.1 Sample Preparations

^{241}Am was purified and quantified as described previously [24, 27]. All sample preparation and experiments were conducted in a restricted area for radioactive materials, following precautions. Na_2CO_3 (TraceSELECT >99.999%, Sigma-Aldrich, St. Louis, MO, USA) was dried in an oven (285°C) for 1 h before dissolution in Millipore water (MilliQ, Millipore, Billerica, MA, USA). Aliquots of Na_2CO_3 stock solution (0.52 M) were stored at 4°C, and each aliquot was used only once. $NaClO_4$ was purified by recrystallization. Am(III)-CO_3 samples were prepared in an Ar-filled glovebox. Three sets of Am(III)-CO_3 samples were prepared in 1 M $NaClO_4$ in batches, as listed in Table 2. The pH values of the samples were adjusted by adding 0.1 M $HClO_4$ (ULTREX II, Ultrapure reagent, JT Baker, Phillipsburg, NJ, USA) in 1 M $NaClO_4$. The pH values of series C in Table 2 were measured on the preparation day, whereas those of series A and B were measured on 65th and 50th days after the preparations, respectively. The pH was measured using a glass combination electrode (Orion™, Ross Ultra, Thermo Fisher Scientific, Waltham, MA, USA) and corrected for changes in the junction potential and activity of H^+ in 1 M $NaClO_4$ by adding an experimentally measured correction factor of 0.26. The correction factor of the electrode was determined from the average deviations of the measured pH values of the $HClO_4$ solutions from the known H^+ concentrations (10^{-3} to 10^{-2} M) in 1 M $NaClO_4$ [30-31].

Table 2. List of test samples

A: Am 11.3 μM + Na_2CO_3 20 mM		B: Am 5.9 μM + Na_2CO_3 20 mM		C: Am 0.52 μM + Na_2CO_3 18 mM	
Sample	pHc*	Sample	pHc*	Sample	pHc*
A0**	< 3	B0**	< 3	C0**	2.40
A1	10.06	B1	10.55	C1	10.23
A2	9.60	B2	10.11	C2	9.83
A3	8.83	B3	9.58	C3	9.50
A4	8.50	B4	9.08	C4	9.24
A5	8.08	B5	8.96	C5	8.89
		B6	7.79	C6	8.23
		B7	8.03	C7	7.41
				C8	7.16
				C9	9.06
				C10	8.63

*pHc ($-\log[H^+]$) = $pH_{measured}$ + 0.26
**In the absence of Na_2CO_3

2.2 UV-Vis Spectrophotometry

The absorption spectra were acquired with a spectrophotometer (Cary 5000, Agilent Technologies, Santa Clara, CA, USA) equipped with a temperature controller (deviation < ± 0.2°C). Quartz cells with a beam path length of 1 cm were used for sample series A and B, whereas a liquid wave-guided capillary cell (LWCC) (WPI, Sarasota, FL, USA) with a beam path length of 100 cm was used for sample series C. The LWCC was used as described in our previous study [28]. The absorption was scanned in the range of 525–495 nm with a spectral resolution of 0.1 nm, a spectral bandwidth of 0.5 nm, and an average time of 1 s. Absorption spectra were deconvoluted using HypSpec software (HypSpec, Version 1.1.16; Protonic Software, Hanau, Germany).

2.3 TRLFS

The luminescence spectra and lifetimes of Am(III)-CO_3 samples were acquired using a TRLFS system [27, 32]. An Nd-YAG pumped optical parametric oscillator system (Vibrant B, Opotek, Carlsbad, CA, USA) was employed as a wavelength-tunable nanosecond pulsed laser source. The excitation wavelength was selected between 503.0–507.3 nm (3.0–3.8 mJ) as per the maximum absorption wavelength (λ_{max}) of each sample. Emissions were detected using an intensified charge-coupled device (iStar, Andor Technology, Belfast, UK) attached to a spectrograph (SR-303i, Andor Technology). Luminescence decay rates were measured as the consecutive delays of intensified charge-coupled device gate opening with a 5-ns step. All measurements were conducted at 25°C and controlled by a thermostat (Q-pod, Quantum Northwest, Seattle, WA, USA).

3. Results and Discussion

3.1 Simulations of Am(III)-CO_3 Species Distribution

The species distribution of Am(III) was simulated for 11.3 μM Am(III) in the presence of 20 mM Na_2CO_3 and for 0.52 μM Am(III) in the presence of 18 mM Na_2CO_3 in 1 M $NaClO_4$ using the computation program Aq_Solutions (Academic Software, UK, www.acadsoft.co.uk). Concentrations of 11.3 and 0.52 μM Am(III) were chosen because they are in the ranges of the minimum concentrations that can be detected in UV-Vis spectrophotometry with a 1-cm quartz cell and 100-cm LWCC, respectively, considering the molar absorption coefficient of free aqua Am^{3+} (424 ± 8 $M^{-1}\cdot cm^{-1}$) [24, 27]. Na_2CO_3 concentrations of 15–20 mM are the experimentally determined minimal concentration ranges at which one or more aqueous Am(III)-CO_3 complexes can be stably formed. The equilibrium constants used in the simulations are listed in Table 1. For solid Am(III) carbonates, thermodynamic data for only the amorphous states were included in the calculations because amorphous solids are typically formed in the initial stage of precipitation.

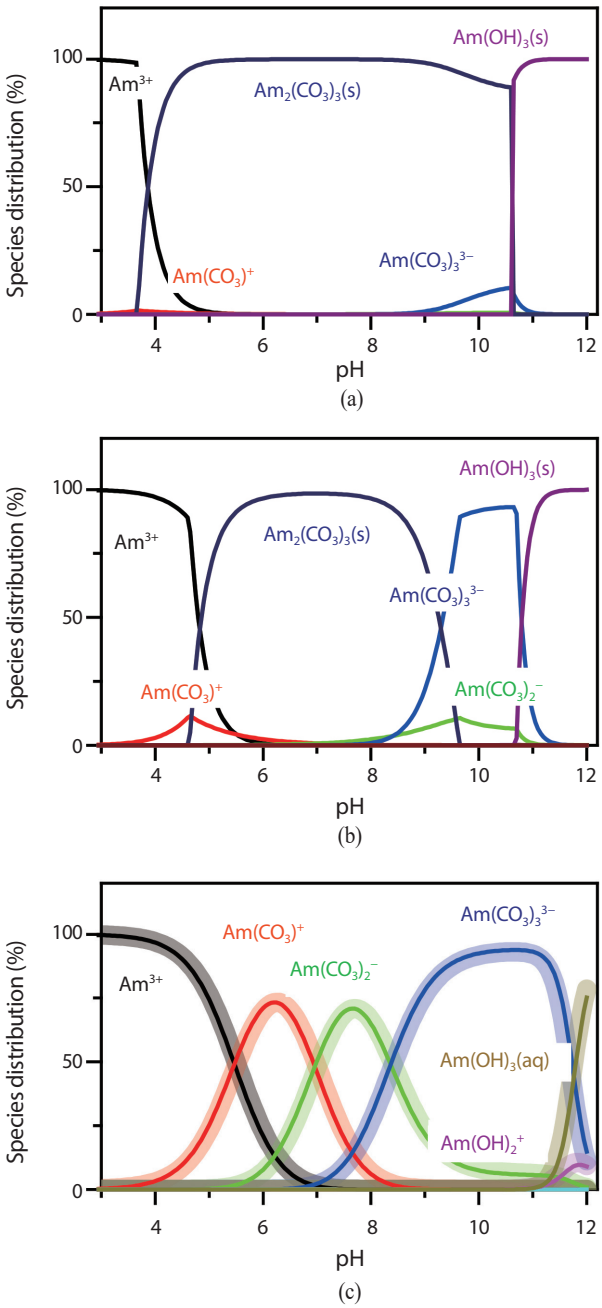

Fig. 1. pH-dependent species distribution of (a) 11.3 μM Am(III) and 20 mM Na_2CO_3 and (b) 0.52 μM Am and 18 mM Na_2CO_3 in 1 M $NaClO_4$. Of the solid states listed in Table 1, only the amorphous states of $Am_2(CO_3)_3$(am), $AmCO_3OH$(am, hyd), $Am(OH)_3$(am) were included in the calculations. (c) Aqueous species distributions for 11.3 μM (thin solid lines) and 0.52 μM (thick transparent lines) Am(III) excluding solid states. Equilibrium constants of the aqueous species are listed in Table 1.

In addition, the reported solubility data for crystalline solids are too low to explain the experimental results below. The thermodynamic constants under standard conditions (I = 0, 25°C) were converted to those under the experimental conditions used in this study (I = 1 M $NaClO_4$, 25°C) according to the specific ion interaction theory, with binary ion interaction coefficients selected in OECD-NEA chemical thermodynamics [2].

Fig. 1(a) shows the simulation results for 11.3 μM Am(III) in 20 mM Na_2CO_3. In the wide pH range of 4–10.5, the solid $Am_2(CO)_3$(am) compound appeared to be predominant. Above pH 10.5, $Am(OH)_3$(am) was the major species. Only approximately 10% of Am(III) appeared as an aqueous $Am(CO_3)_3^{3-}$ complex at pH 10.5. Fig. 1(b) shows the simulation results for 0.52 μM Am(III) in the presence of 18 mM Na_2CO_3. Compared with 11.3 μM Am(III), the $Am_2(CO_3)_3$(am) compound was predominant in a slightly narrower pH range of 5–9, and the aqueous $Am(CO_3)_3^{3-}$ complex appeared as the major species at pH 10. Above pH 11, $Am(OH)_3$(am) was the predominant species. When the solid compounds were excluded from the calculations, the simulation results showed that aqueous complexes of $Am(CO_3)^+$, $Am(CO_3)_2^-$, and $Am(CO_3)_3^{3-}$ appeared in series as the predominant species at pH 5.5–7, 7–8.5, and 8.5–11, respectively, for both Am(III) concentrations of 11.3 μM (thin solid lines) and 0.52 μM (thick transparent lines) in Fig. 1(c).

3.2 UV-Vis Absorption Spectra of Am(III)-CO_3 and Sample Aging Effects

The absorption spectra of 11.3 μM Am(III) were measured in the presence of 20 mM Na_2CO_3 at various pH values between 8 and 10 (A series in Table 2). The samples were prepared in 1-cm quartz cells with sealing caps and stored in these cells throughout the monitoring period. Fig. 2 shows the absorption spectra of fresh samples, which were prepared 2 h before the measurements. The positions of the absorption peaks were sequentially red-shifted as the pH increased. Regardless of the pH, the absorbance

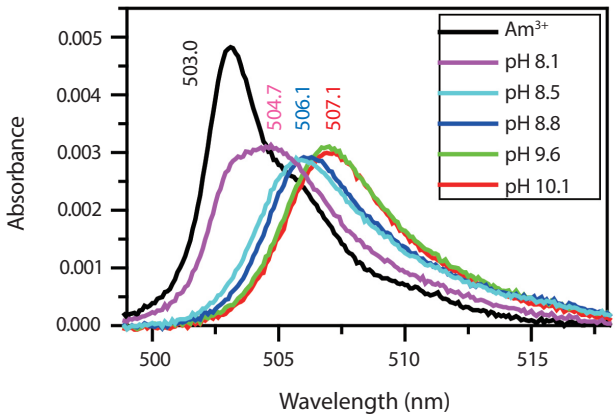

Fig. 2. pH-dependent absorption spectra of 11.3 μM Am in the presence of 20 mM Na_2CO_3 in 1 M $NaClO_4$. Spectra were acquired at 2 h after sample preparation. The absorption spectrum of Am^{3+} was obtained in the absence of Na_2CO_3 as a reference at pH 3 (black).

of Am(III) in the carbonate solutions was similar, and the molar absorbance was lower than that of free Am^{3+}.

According to the simulation results presented in Fig. 1(a), $Am_2(CO_3)_3$(am) was predicted to be the predominant species under our experimental conditions of 11.3 μM Am(III) with 20 mM Na_2CO_3 at pH 8–10, suggesting that solid states formed in the samples. The absorption spectra were monitored periodically over two months to evaluate whether the observed absorption was due to colloidal particles. Fig. 3 shows the representative aging time-dependent absorption spectral changes of the samples under the three different pH conditions. In Fig. 4, the overall absorbance changes are plotted as a function of the sample aging time. The instrumental conditions were confirmed to be stable based on the constant absorption spectra of Am^{3+} throughout the monitoring period (Fig. 3(a)).

Samples at pH below 9.5 showed a gradual decrease in absorbance along with shifts in the peak positions that finally converged to ~506 nm (Figs. 3(b) and 3(c)). Such gradual changes in the absorption spectra during aging indicate the involvement of solid states, which are likely colloidal particles, which formed slowly during the monitoring period. Approximately one month was required for the test samples to reach an apparent chemical equilibrium (Fig. 4).

However, samples above pH 9.5 showed no considerable change in the absorption spectra (Fig. 3(d)). According to the simulation results, excluding the solid state (shown in Fig. 1(c)), $Am(CO_3)_3^{3-}$ was the major species at pH values above 9.5. The stable absorption spectra over two months indicate that solid compounds, which typically induce spectral changes over time, were not present in the samples. Only the aqueous complex, presumably $Am(CO_3)_3^{3-}$, was the major species under these conditions (11.3 μM Am(III),

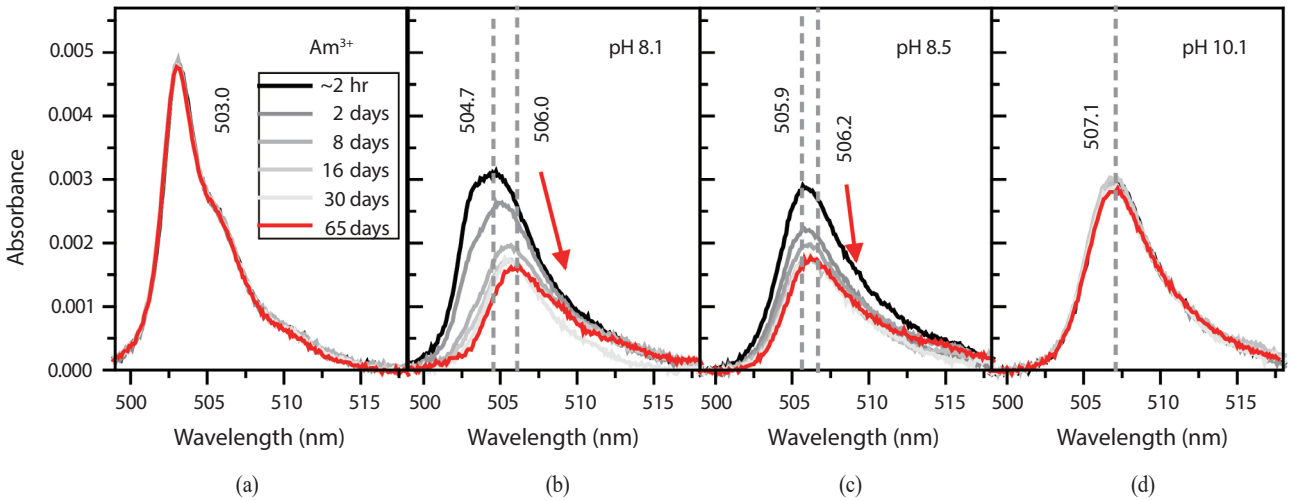

Fig. 3. Aging effects of the absorption spectra of 11.3 μM Am(III) samples in the absence (a) and presence of 20 mM Na_2CO_3 (b)–(d) (A series in Table 2).

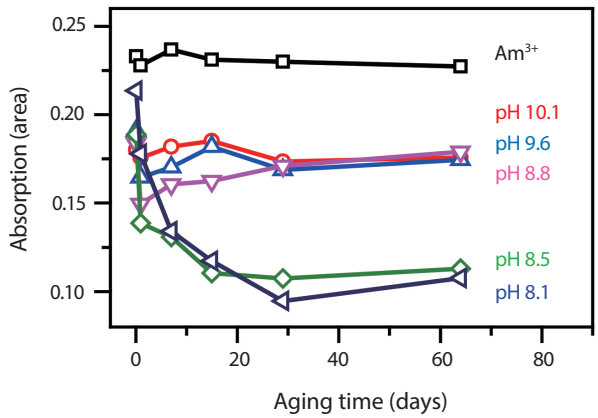

Fig. 4. Aging time-dependent absorption changes (absorption area of 505–515 nm) of 11.3 μM Am(III) in the presence of 20 mM Na_2CO_3 samples (A series in Table 2).

20 mM Na_2CO_3, pH > 9.5). Similar results were observed for samples with 5.9 μM Am(III) (data not shown).

We found that solid compounds were less prone to form under our experimental conditions (series A−C), indicating higher solubilities than those predicted in the simulations. Notably, the simulations in Fig. 1 include only amorphous solid compounds. When crystalline compounds that exhibit much lower solubility were included, the discrepancies increased. The discrepancy between the experimental results and simulation results suggests that the reported solubility constants, which are associated with large uncertainties as described in the Introduction, should be applied cautiously. Particularly, if the process of solid-state formation is associated with relatively slow reaction steps, for example because of the high activation energy required to overcome the transition to the solid state, reaction kinetics can control the species distributions under specific conditions. Our results suggest that reaction systems involving the formation or transformation of solid states are often not well-described by thermodynamic equilibrium constants alone; their kinetic parameters must be considered when predicting radionuclide migration.

3.3 Luminescence Properties

Fig. 5(a) shows the luminescence spectra of 11.3 μM Am(III) in the presence of 20 mM Na_2CO_3 (series A). The spectra were measured on day three after sample preparation. Compared to the luminescence properties of Am^{3+} (luminescence peak at 688 nm, lifetime of 23.3 ± 0.4 ns) [24, 27], the luminescence spectrum of the pH 10.1 sample shifted to

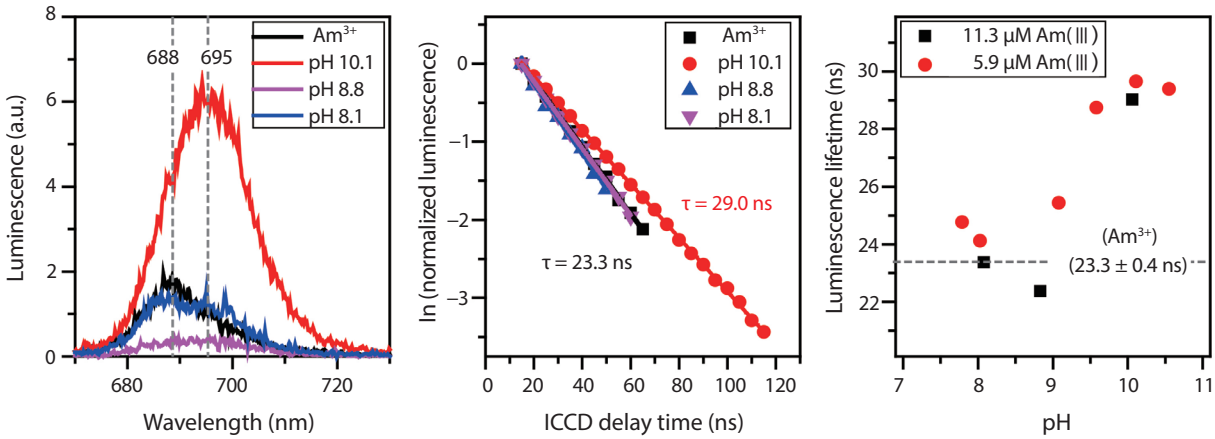

(a) (b) (c)

Fig. 5. Luminescence properties of Am(III)-CO_3 (a) Representative luminescence spectra and (b) luminescence decay plots of 11.3 μM Am(III) in the presence of 20 mM Na_2CO_3 (A series). Measurements were conducted on day three after sample preparation. The maximum absorption wavelength of each sample was employed for the excitation wavelength. (c) Summary of pH-dependent luminescence lifetimes of 11.3 and 5.9 μM Am(III) samples (A and B series in Table 2).

695 nm with significantly enhanced luminescence intensity (Fig. 5(a)). The luminescence lifetime increased to ~29 ns (Fig. 5(b)). The luminescence lifetimes of the 11.3 and 5.9 μM Am(III) samples (series A and B) are plotted as a function of pH in Fig. 5(c). Samples with a pH above 9.5, whose predominant species were likely aqueous $Am(CO_3)_3^{3-}$ complexes, consistently showed luminescence lifetimes of approximately 30 ns. These results are consistent with those reported in a TRLFS study of Am(III)-carbonate systems by Runde et al., which also showed that the luminescence spectrum of the aqueous $Am(CO_3)_3^{3-}$ complex shifts to 694.6 nm with an extended luminescence lifetime of 34.5 ± 2.4 ns [29]. The observed red-shifted luminescence and absorption spectra were ascribed to the strong ligand field splitting by ligand binding. The enhanced luminescence with elongated lifetimes of ligand-bound Am(III) occurred because of the reduced number of inner-sphere bound H_2O molecules ($n(H_2O)$), whose OH vibrations quenched the luminescence [33-34]. These are well-known phenomena observed for trivalent ions, such as Cm(III) and Eu(III) [15, 19, 29] as well as Am(III) [27-28].

For the Am(III) ion, the relationship between the luminescence lifetime (τ) and $n(H_2O)$ was estimated as $n(H_2O) \pm 0.5 = 2.56 \times 10^{-7} \cdot (1/\tau) - 1.43$ by Kimura et al. [34]. According to this equation, luminescence lifetimes of 30–34 ns correspond to the displacement of approximately 2.5–3.5 H_2O molecules on average from the inner-sphere of the Am(III) ion. These values are too low for the $Am(CO_3)_3^{3-}$ complex, which is thought to displace six H_2O molecules in total, considering that carbonate ions typically interact with a metal center in a bidentate mode [13, 19, 35]. These results show that the Am(III)-carbonate system was not well-fitted by the equation proposed by Kimura et al., unlike the Cm(III)- and Eu(III)-carbonate systems, which are fairly well-explained by the established relationships [15, 19, 29]. Further studies of Am(III) systems are needed to understand the distinctive spectroscopic properties of Am(III)-CO_3 complexes in more detail.

The pH 8.8 sample showed reduced luminescence inten-

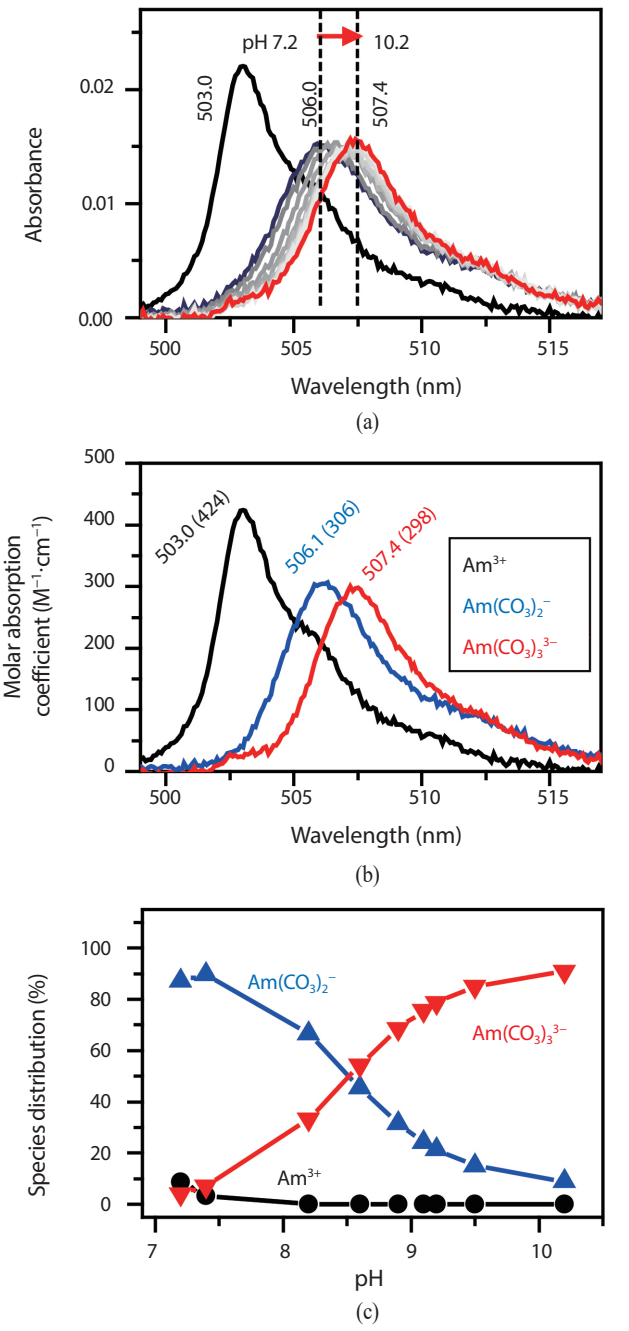

Fig. 6. Absorption spectra 0.52 μM Am(III) in the presence of 18.2 mM Na_2CO_3 in 1 M $NaClO_4$ (a) pH-dependent absorption spectra of the series C. As a reference, the absorption spectrum of 0.52 μM Am^{3+} in 1 M $NaClO_4$ and pH 2.4 in the absence of Na_2CO_3 is plotted in black. A LWCC (100 cm beam path-length) was used for the measurements. (b) Deconvoluted absorption spectra of $Am(CO_3)_2^-$ and $Am(CO_3)_3^{3-}$ complexes. Values in parentheses are the molar absorption coefficients. (c) Species distribution of Am(III)-CO_3 complexes estimated from the deconvolution.

sity but no change in the luminescence lifetime (Figs. 5(a) and 5(b)). We previously observed similar results for colloidal $Am(OH)_3$(s) particles, which were characterized by an absorption peak at 506 nm but no luminescence [24, 27]. The same properties were observed for $Am_2(oxalate)_3$(s) (data not shown). These consistent observations from the three different systems suggest that Am(III) colloidal particles are characterized by absorption at approximately 506 nm but have non-luminescent properties.

3.4 Absorption Spectra of Aqueous Am(III)-CO_3 Complexes

To determine the absorption spectra of aqueous Am(III)-CO_3 complexes, we performed experiments at a lower concentration of Am(III) (0.52 μM) in the presence of 18 mM Na_2CO_3. Samples were prepared at various pH values of 7.2–10.2. The absorption spectra of fresh samples prepared 2 h before the measurements were conducted in a 100-cm LWCC. As the pH was increased from 7.2 to 10.2, the absorption spectra of Am(III) gradually red-shifted from 506.0 to 507.4 nm (Fig. 6(a)), similar to the results observed for 11.3 μM Am(III) (Fig. 2). As described in the section 3.2 for the sample aging effect, colloidal formation was likely in the initiation stage by the time of the measurements, and Am(III) was mainly present as an aqueous species at pH 7.2–9.0. Thus, the observed sequentially red-shifted absorption spectra were primarily from aqueous complexes.

Assuming that solid Am(III) compounds were not present in the samples, the absorption spectra were deconvoluted. Factor analysis suggested that the observed changes in the absorption spectra were best-described by a mixture of $Am(CO_3)_2^-$ and $Am(CO_3)_3^{3-}$ in addition to Am^{3+}. The deconvoluted individual absorption spectra of the $Am(CO_3)_2^-$ and $Am(CO_3)_3^{3-}$ complexes were identified at 506.1 and 507.4 nm, respectively (Fig. 6(b)) with estimated molar absorption coefficients of approximately 306 and 298 $M^{-1}\cdot cm^{-1}$, respectively, which were lower than those of Am^{3+} (424 ± 8 $M^{-1}\cdot cm^{-1}$). $Am(CO_3)^+$ was not detected under these conditions. Previous LPAS studies of Am(III)-carbonate systems reported similar results, where the absorption spectra of $Am(CO_3)_2^-$ and $Am(CO_3)_3^{3-}$ complexes were assigned to positions similar to those in our results, and the molar absorption coefficients of 350.1 and 334.1 $M^{-1}\cdot cm^{-1}$, respectively, gradually decreased for the complexes [17, 26].

The species distribution was determined from the deconvolution (Fig. 6(c)); the estimated formation constants were $\log\beta\,(1, 2) = 9.30 \pm 0.02$ and $\log\beta\,(1, 3) = 12.13 \pm 0.03$. Notably, these values are rough estimations from a single experiment under the assumption that the reaction solutions contained only aqueous species. However, the values are in a reasonable range based on those reported in the OECD NEA review ($\log\beta\,(1, 2) = 10.11 \pm 0.6$, $\log\beta\,(1, 3) = 13.04 \pm 0.5$ in I = 1.0 M $NaClO_4$). These results indicate that the deconvoluted spectra of each Am(III)-CO_3 species were acceptable. The absorption spectra of each Am(III)-CO_3 species can be used as references for further studies of more complicated systems, such as ternary Ca-Am-CO_3 complexes.

4. Conclusions

The absorption spectra of $Am(CO_3)_2^-$ and $Am(CO_3)_3^{3-}$ complexes were identified at 506.1 and 507.4 nm, respectively. The molar absorption coefficients of these complexes were lower (approximately 300 $M^{-1}\cdot cm^{-1}$) than that of the free aqueous Am^{3+} (503.0 nm, 424 ± 8 $M^{-1}\cdot cm^{-1}$). The aqueous $Am(CO_3)_3^{3-}$ complex was stable at approximately pH 9.5 for [Am(III)] ≤ 11.3 μM in the presence of [Na_2CO_3] ≥ 18 mM in 1 M $NaClO_4$. The luminescence spectrum of the $Am(CO_3)_3^{3-}$ complex was observed at 695 nm, with significantly enhanced luminescence and an extended lifetime of approximately 30 ns. In contrast, Am(III)-carbonate colloidal particles were distinct from aqueous complexes because of their characteristic absorption at approximately 506 nm but had non-luminescent properties. The slow

formation of colloidal Am(III)–carbonate particles was monitored for over a month, after which these particles remained stable for at least another month. The experimentally observed species distribution did not follow the simulated results based on the equilibrium constants in OECD NEA reviews; aqueous Am(III)-carbonate species were detected over the predicted solubility limits, possibly because of the presence of kinetic barriers for the formation of solid compounds. Our results suggest that the kinetic parameters and equilibrium constants should be considered together when assessing radionuclide migration. The absorption and luminescence properties of the Am(III)-carbonate complexes can be used as reference data for further studies on carbonates such as complex ternary systems of Ca-Am(III)-CO_3 and will enable tracking of time-dependent species evolution.

Acknowledgements

This research was supported by the Nuclear Research and Development Program of the National Research Foundation of Korea (Nos. 2021M2E1A1085202 and 2022M2D2A1A02063990).

Disclosure and conflicts of interests

There are no conflicts to declare.

REFERENCES

[1] J.I. Kim, "Significance of Actinide Chemistry for the Long-Term Safety of Waste Disposal", Nucl. Eng. Technol., 38, 459-482 (2006).

[2] I. Grenthe, X. Gaona, A.V. Plyasunov, L. Rao, W.H. Runde, B. Grambow, R.J.M. Konings, A.L. Smith, and E.E. Moore. Chemical Thermodynamics Vol. 14: Second Update on the Chemical Thermodynamics of Uranium, Neptunium, Plutonium, Americium, and Technetium, OECD Nuclear Energy Agency Report (2020).

[3] Z. Wang, J.M. Zachara, W. Yantasee, P.L. Gassman, C. Liu, and A.G. Joly, "Cryogenic Laser Induced Fluorescence Characterization of U(VI) in Hanford Vadose Zone Pore Waters", Environ. Sci. Technol., 38(21), 5591-5597 (2004).

[4] G. Bernhard, G. Geipel, V. Brendler, and H. Nitsche, "Speciation of Uranium in Seepage Waters of a Mine Tailing Pile Studied by Time-Resolved Laser-Induced Fluorescence Spectroscopy (TRLFS)", Radiochim. Acta, 74(s1), 87-91 (1996).

[5] Y. Jo, H.R. Cho, and J.I. Yun, "Visible-NIR Absorption Spectroscopy Study of the Formation of Ternary Plutonyl(VI) Carbonate Complexes", Dalton Trans., 49(33), 11605-11612 (2020).

[6] M.H. Baik, E.C. Jung, and J. Jeong, "Determination of Uranium Concentration and Speciation in Natural Granitic Groundwater Using TRLFS", J. Radioanal. Nucl. Chem., 305(2), 589-598 (2015).

[7] E.C. Jung, M.H. Baik, H.R. Cho, H.K. Kim, and W. Cha, "Study on the Interaction of U(VI) Species With Natural Organic Matters in KURT Groundwater", J. Nucl. Fuel Cycle Waste Technol., 15(2), 101-116 (2017).

[8] J.Y. Lee and J.I. Yun, "Formation of Ternary $CaUO_2(CO_3)_3^{2-}$ and $Ca_2UO_2(CO_3)_3$(aq) Complexes Under Neutral to Weakly Alkaline Conditions", Dalton Trans., 42(27), 9862-9869 (2013).

[9] Y. Jo, A. Kirishima, S. Kimuro, H.K. Kim, and J.I. Yun, "Formation of $CaUO_2(CO_3)_3^{2-}$ and $Ca_2UO_2(CO_3)_3$(aq) Complexes at Variable Temperatures (10–70°C)", Dalton Trans., 48(20), 6942-6950 (2019).

[10] Z. Zheng, T.K. Tokunaga, and J. Wan, "Influence of Calcium Carbonate on U(VI) Sorption to Soils", Environ. Sci. Technol., 37(24), 5603-5608 (2003).

[11] W. Dong, W.P. Ball, C. Liu, Z. Wang, A.T. Stone, J. Bai, and J.M. Zachara, "Influence of Calcite and Dissolved Calcium on Uranium(VI) Sorption to a Hanford

Subsurface Sediment", Environ. Sci. Technol., 39(20), 7949-7955 (2005).

[12] S.C. Brooks, J.K. Fredrickson, S.L. Carroll, D.W. Kennedy, J.M. Zachara, A.E. Plymale, S.D. Kelly, K.M. Kemner, and S. Fendorf, "Inhibition of Bacterial U(VI) Reduction by Calcium", Environ. Sci. Technol., 37(9), 1850-1858 (2003).

[13] R. Guillaumont, T. Fanghänel, V. Neck, J. Fuger, D. Palmer, I. Grenthe, and M.H. Rand, Chemical Thermodynamics Vol. 5: Update on the Chemical Thermodynamics of Uranium, Neptunium, Plutonium, Americium, and Technetium, Elsevier, Amsterdam (2003).

[14] R. Lundqvist, "Hydrophilic Complexes of the Actinides. I. Carbonates of Trivalent Americium and Europium", Acta Chem. Scand., A36, 741-750 (1982).

[15] T. Vercouter, P. Vitorge, B. Amekraz, E. Giffaut, S. Hubert, and C. Moulin, "Stabilities of the Aqueous Complexes $Cm(CO_3)_3^{3-}$ and $Am(CO_3)_3^{3-}$ in the Temperature Range 10−70°C", Inorg. Chem., 44(16), 5833-5843 (2005).

[16] A.R. Felmy, D. Rai, and R.W. Fulton, "The Solubility of $AmOHCO_3$(c) and the Aqueous Thermodynamics of the System Na^+-Am^{3+}-HCO_3^--CO_3^{2-}-OH^--H_2O", Radiochim. Acta, 50(4), 193-204 (1990).

[17] G. Meinrath and J.I. Kim, "The Carbonate Complexation of the Am(III) Ion", Radiochim. Acta, 52-53(1), 29-34 (1991).

[18] H. Nitsche and E.M. Standifer, "Americium(lll) Carbonate Complexation in Aqueous Perchlorate Solution", Radiochim. Acta, 46(4), 185-190 (1989).

[19] J.I. Kim, R. Klenze, H. Wimmer, W. Runde, and W. Hauser, "A Study of the Carbonate Complexation of Cm^{III} and Eu^{III} by Time-resolved Laser Fluorescence Spectroscopy", J. Alloys. Compd., 213-214, 333-340 (1994).

[20] Th. Fanghänel, H.T. Weger, Th. Könnecke, V. Neck, P. Paviet-Hartmann, E. Steinle, and J.I. Kim, "Thermodynamics of Cm(III) in Concentrated Electrolyte Solutions. Carbonate Complexation at Constant Ionic Strength (1 m NaCl)", Radiochim. Acta, 82(s1), 47-53 (1998).

[21] Th. Fanghänel, Th. Könnecke, H. Weger, P. Paviet-Hartmann, V. Neck, and J.I. Kim, "Thermodynamics of Cm(III) in Concentrated Salt Solutions: Carbonate Complexation in NaCl Solution at 25°C", J. Solution Chem., 28(4), 447-462 (1999).

[22] T. Vercouter, P. Vitorge, N. Trigoulet, E. Giffaut, and C. Moulin, "$Eu(CO_3)_3^{3-}$ and the Limiting Carbonate Complexes of Other M^{3+} f-elements in Aqueous Solutions: A Solubility and TRLFS Study", New J. Chem., 29(4), 544-553 (2005).

[23] V. Philippini, T. Vercouter, and P. Vitorge, "Evidence of Different Stoichiometries for the Limiting Carbonate Complexes Across the Lanthanide(III) Series", J. Solution Chem., 39(6), 747-769 (2010).

[24] H.K. Kim, H.R. Cho, E.C. Jung, and W. Cha, "Radioanalytical and Spectroscopic Characterizations of Hydroxo- and Oxalato-Am(III) Complexes", J. Nucl. Fuel Cycle Waste Technol., 16(4), 397-410 (2018).

[25] T.K. Keenan, "Americium and Curium", J. Chem. Educ., 36(1), 27-31 (1959).

[26] R. Klenze, J.I. Kim, and H. Wimmer, "Speciation of Aquatic Actinide Ions by Pulsed Laser Spectroscopy", Radiochim. Acta, 52-53, 97-103 (1991).

[27] H.K. Kim, K. Jeong, H.R. Cho, E.C. Jung, K. Kwak, and W. Cha, "Spectroscopic Speciation of Aqueous Am(III)–Oxalate Complexes", Dalton Trans., 48(27), 10023-10032 (2019).

[28] H.K. Kim, K. Jeong, H.R. Cho, K. Kwak, E.C. Jung, and W. Cha, "Study of Aqueous Am(III)-Aliphatic Dicarboxylate Complexes: Coordination Mode-Dependent Optical Property and Stability Changes", Inorg. Chem., 59(19), 13912-13922 (2020).

[29] W. Runde, C. Van Pelt, and P.G. Allen, "Spectroscopic Characterization of Trivalent f-element (Eu, Am) Solid Carbonates", J. Alloys Compd., 303-304, 182-190 (2000).

[30] S. Cho, H.K. Kim, T.H. Kim, W. Cha, and H.R. Cho,

"Thermodynamic Studies on the Hydrolysis of Trivalent Plutonium and Solubility of $Pu(OH)_3(am)$", Inorg. Chem., 61(32), 12643-12651 (2022).

[31] N. Jordan, M. Demnitz, H. Lösch, S. Starke, V. Brendler, and N. Huittinen, "Complexation of Trivalent Lanthanides (Eu) and Actinides (Cm) With Aqueous Phosphates at Elevated Temperatures", Inorg. Chem., 57(12), 7015-7024 (2018).

[32] E.C. Jung, H.R. Cho, M.H. Baik, H. Kim, and W. Cha, "Time-resolved Laser Fluorescence Spectroscopy of $UO_2(CO_3)_3^{4-}$", Dalton Trans., 44(43), 18831-18838 (2015).

[33] W.D. Horrocks and D.R. Sudnick, "Lanthanide Ion Probes of Structure in Biology. Laser-induced Luminescence Decay Constants Provide a Direct Measure of the Number of Metal-coordinated Water Molecules", J. Am. Chem. Soc., 101(2), 334-340 (1979).

[34] T. Kimura and Y. Kato, "Luminescence Study on Determination of the Inner-Sphere Hydration Number of Am(III) and Nd(III)", J. Alloys Compd., 271-273, 867-871 (1998).

[35] C. Priest, Z. Tian, and D. Jiang, "First-Principles Molecular Dynamics Simulation of the $Ca_2UO_2(CO_3)_3$ Complex in Water", Dalton Trans., 45(24), 9812-9819 (2016).